

Optimizing the Intersection Region Performance for LHC

Peter McIntyre and Akhdiyov Sattarov
Texas A&M University

Each high-luminosity intersection region at LHC poses significant challenges for the match of the physics mission of the collider with the optical train of the arcs. Largely speaking there are three sets of issues that must be respected in IR design: focal optics, crossing and separation of the two beams, and management of secondary particles produced in proton-proton interactions at the beam crossing. The focal optics required for the symmetric squeeze of symmetric beams is a quadrupole triplet. A pair of dipoles are used to bring the beams must be brought into a crossing geometry from their displaced arcs. Because the focal length at the IR is >100 times less than that in the arcs, it is important to correct chromaticity that arises in the IR locally so that it does not require global correction through the arcs where there limited pole strength is available in the families of sextupoles. The effects of multipole errors and misalignments in the focal elements of the IR optics grow rapidly with the spacing of those elements from the IR. For both of these reasons an optimal geometry would place the quadrupole triplet as close as possible to the beam crossing.

Because the separation of bunches in the circulating beams is smaller than the overall length of the optical train that crosses and separates the beams, subsidiary bunch-bunch crossings will produce tune shift and spread, and beam-beam interactions between partially separated beams produce asymmetric lensing. For this reason it is desirable to fully separate the two beams as close to the intersection point (IP) as possible. The placement of the dipoles and quadrupoles in these respects compete in optimizing the crossing optics.

Finally the flux of particles produced in the forward directions in the proton-proton interactions at the crossing must be handled in a way that minimizes background albedo in the detectors. These forward particles carry a great deal of energy and many of them inevitably will end up in the coils and structure of the first elements of the IR optical train. Those ‘first wall’ elements must be built with provisions for minimizing cryogenic heat load, maximizing heat transport, and accommodating radiation damage to the insulating materials.

Earlier studies of options for upgrading the IR optics for increasing luminosity have taken as starting assumptions that the IR optics must be located beyond the boundary between each detector and the IR optics, negotiated to be $s = 21$ m. Such a constraint is a heavy penalty because it impacts the attainable β^* , the magnitude of β_{\max} in the triplet, the impact on chromaticity, and the sensitivity to multipoles in the IR elements. For these reason we have instead chosen to place the quadrupole triplet within the aperture of the actual detector, beginning as close as possible to the IP and minimizing its transverse size and its magnetic coupling to the magnets of the detector itself. Such placement may or may not be possible depending upon the requirements for this hard-forward region for detector systems. Decisions on potential conflict can best be made by once the importance of this region for attaining maximum luminosity is appreciated.

In each of the two large detectors there are plans to extend the physics reach down to the hard-forward direction, particularly in the effort to detect signals from diffractive production of the Higgs boson. Preliminary discussions indicate, however, that it is projected that some of the detector elements in this direction will have limited life and usefulness once high luminosity is achieved. In designing an IR upgrade to maximize luminosity, a cylindrical region beginning ~ 12 m from the IP, with a radius of ~ 15 cm, could be considered for IR optics if it produced a significant gain in luminosity without complicating albedo backgrounds into the forward detector elements. In this paper, we consider an optimization of the IR optics in which the quadrupole triplet begins at $s = 12$ m, and the separation dipoles follow the triplet. The placement of the elements in the optical train are shown in Figure 1.

The first quadrupole (Q_1) in the triplet and the first dipole in the separator (D_1) must absorb the radiation dose and heat produced by secondary particles produced in collisions. Whereas the baseline IR design places these elements beyond the detector region and behind massive shielding, the optimization considered here places them more directly in harm's way. To appreciate the magnitude of this problem, consider the forward spectrum of particles, primarily from diffraction.

We assume the design luminosity $\mathcal{L} = 10^{34} \text{ cm}^{-2}\text{s}^{-1}$, a total cross section $\sigma_{\text{tot}} = 10^{25} \text{ cm}^2$, and a pseudorapidity density $\frac{dn}{d\eta}$ and transverse momentum (p_t) distribution shown in Figure 2.

For an angular region $\theta_1 < \theta < \theta_2$, particles contribute energy in proportion to $dE \sim dp_t/\theta$ and the total intercepted power is

$$P_{Q_1} \sim L \sigma_{\text{tot}} \langle p_t \rangle \int_{\theta_1}^{\theta_2} \frac{dn}{d\eta} \frac{d\eta}{\theta}$$

The heat loads estimated in this way for high-luminosity operation for the first four magnets of the IR are given in Table 1.

It will of course be necessary to simulate the heat loads and the distribution of heat in each magnet using the particle-in-cell codes of Mokhov [1].

Q_1 must operate with a heat load that is probably greater than can be sustained with a conventional coil structure. A quadrupole design appropriate for this requirement is presented in Section 1.

Quadrupoles Q_2 and Q_3 require larger aperture than Q_1 and hence fall largely in its shadow of Q_1 . They present more modest but still significant requirements for radiation damage and heat load and are discussed in Section 2.

Table 1. Estimated particle-loss heating in the IR magnets for the geometry of Figure 1.

Q_1	Q_2	Q_3	D_1	
300	100	50	3,000	W

The first dipole will horizontally sweep many of the most forward (and most energetic) particles from the interactions at the crossings into the side walls of the dipole. Mokhov² has simulated the energy deposition represented by this fluence; for $L = 10^{34} \text{ cm}^{-2} \text{ s}^{-1}$ it corresponds to $P_{D1} \sim 3 \text{ kW}$. A dipole design appropriate for this most extreme requirement is presented in Section 3.

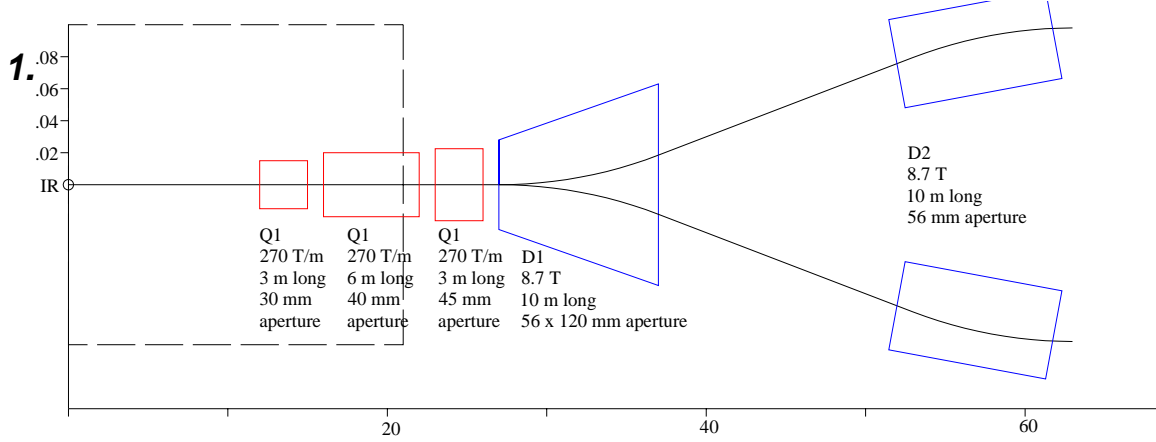


Figure 1. Placement of optical train in optimized IR.

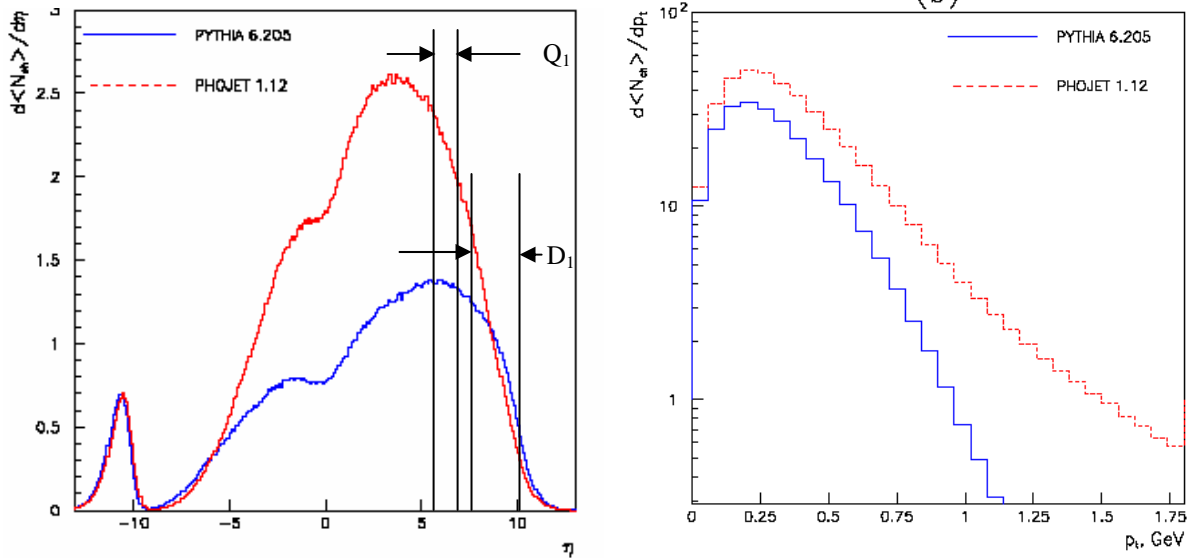


Figure 2. Charged particle multiplicity $dn_{ch}/d\eta$ and p_t distributions for single diffractive fraction, estimated for LHC (Ref. 1). The particle losses to Q_1 and D_1 are indicated.

Q1: Bi-2212 quadrupole for high radiation, high heat load

For this design we examine the case that little shielding is placed in front of Q1 in order to place it as close as possible to the IP. It must absorb the full load of ~ 300 W of particle energy deposition. Such large heat load places extreme requirements on heat transport within the superconducting coil and its structure. In particular it is unlikely that any vacuum-impregnated coil could maintain the limited temperature profile needed for operating Nb₃Sn ($\Delta T \sim 2$ K). The aperture required for Q₁ is similarly reduced in proportion to its distance from the IP: an aperture of ~ 40 mm should be sufficient.

We have developed a quadrupole coil design that would employ to advantage a structured cable [3] containing 6 round strands of superconductor. The cable was developed for use with Bi-2212, in order to provide direct contact of all strands with flowing liquid helium. A cross section of the cable is shown in Figure 3a.

The six strands are arranged in a 6-on-1 cable-in conduit configuration, with the center element being a thin-wall tube made of Inconel X-750. This alloy has the unique property that it can retain spring temper through the reaction heat treat to 870 C in oxygen that is required for the partial-melt anneal of Bi-2212. The cable is inserted within an Inconel 718 outer sheath, then drawn down to preload the spring so that it pushes all 6 strands against the outer sheath.

The point of this cable design is that the spring tube in the core presses each strand against the outer wall and its neighbor strands with a force that is \sim twice the maximum Lorentz force. The strands are then immobilized within the cable, without the requirement of impregnating the interior space between strands and inside the spring tube. This conveys two important advantages. First, it provides for the ability to flow liquid helium through all elements of the cable, so that a coil can be volumetrically cooled just as the coils of Q1 are volumetrically heated by particle energy deposition.

Second, the round cable makes it possible to configure a quadrupole winding that takes best advantage of the smaller aperture required for Q₁. We have demonstrated that when the cable is bent around a small radius of curvature, the strands re-arrange within the cable but each strand retains its round cross-section and is un-strained. Figure 3b shows a test coil having bend radius 7 times the cable radius. When the cable is wrapped around a curvature, both the outer sheath and the spring core deform under strain, but the 6 strands retain their round cross section without deformation. This remarkable property was demonstrated in sections of cable after coil winding, and in critical current tests of test coils such as that in Figure 3b. The coil retained full short-sample current performance. It is therefore possible to wind the coils required for the small aperture of Q1 without straining the cable or losing registration.

The structured cable approach can be used with any of the available superconductors: NbTi (using superfluid helium cooling); Nb₃Sn (using either superfluid helium or supercritical helium cooling); or with Bi-2212 using supercritical helium cooling). The choice will require evaluation of the primary issues of cooling for realistic operation and maximizing the gradient for the required aperture. Examples of all three alternatives are summarized in Table 2.

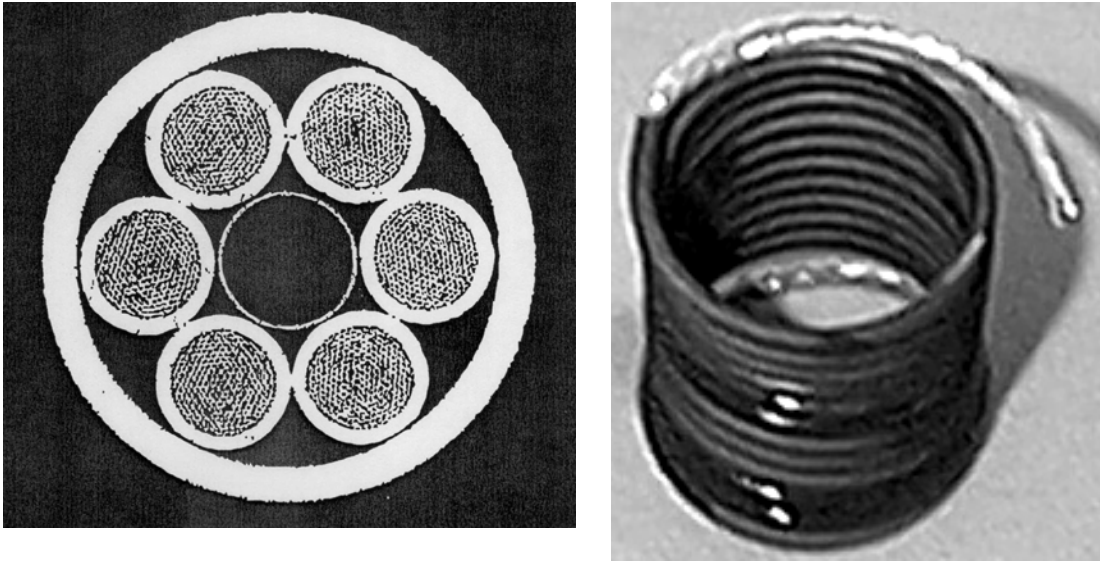


Figure 3. Structured cable containing 6 round multi-filament strands of Bi-2212.

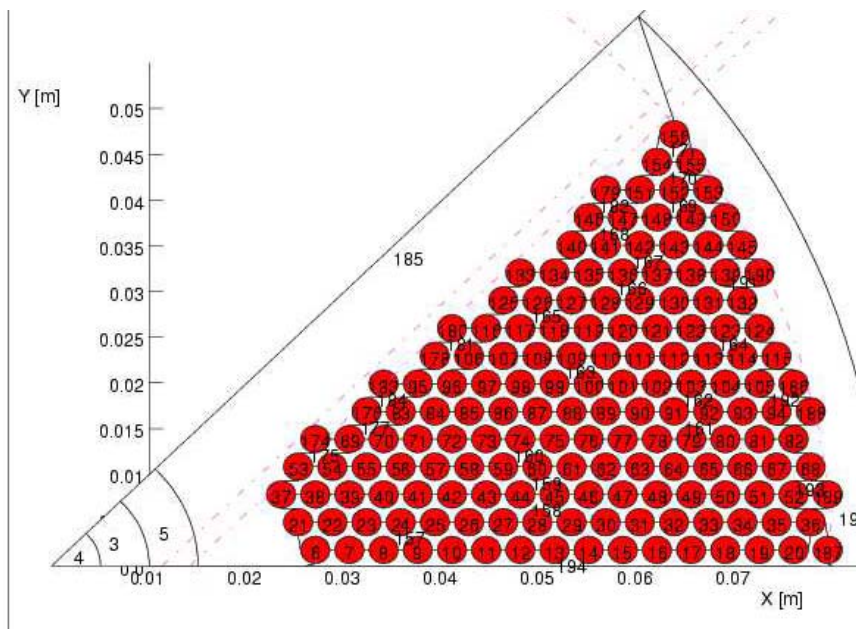


Figure 4. Cross-section of one octant of a structured-coil quadrupole design for Q1.

Table 2. Parameters of Q_1 with 3 alternatives for superconductor.

Superconductor	NbTi	Nb ₃ Sn	Bi-2212	
Stabilizer	Cu (50%)	Cu (50%)	Ag (50%)	
Insulator	Kapton/ Cyanate ester	S-glass/ Cyanate ester	Nextel/ Cyanate ester	
Operating temperature	1.8	4 - 6	10 - 20	K
Strand diameter	1.0	1.0	0.8	mm
Cable spacing	3.5	3.5	2.9	Mm
B_{\max} in windings				T
Strand current			500	A
Gradient				T/m

The coil assembly will be preloaded to about half the working stress level after winding. The Nb_3Sn and Bi-2212 require heat treatment: Nb_3Sn to ~ 650 C, Bi-2212 in a partial melt to ~ 875 C. The case of Bi-2212 is particularly challenging, since the crucial stage of heat treatment is to bring the entire coil into partial melt of the perovskite phase, which entails a brief excursion from $850 \rightarrow 870$ C and back in a time of minutes with a control and uniformity of ~ 1 C. We plan instead to use the isothermal melt processing procedure developed by Holesinger [4], in which the transition to partial melt is controlled by modulating the partial pressure of O_2 in the purge gas.

Cooling of the coil would utilize either superfluid helium (for NbTi or Nb_3Sn) or supercritical helium (for Nb_3Sn or Bi-2212). Flow will be provided by opening channels in the cable elements at their ends where supply and return flow is to be accommodated. These holes would be drilled in the Inconel sheath before the cable was made, at intervals determined by fabrication of a dummy coil to be correct so that each hole is where it is supposed to appear in the end geometry. Note that because the cable contains its own structure, the transfer of axial forces at the ends should be effected more easily than with a coil employing Rutherford cable.

Either choice of superfluid or supercritical helium cooling will entail careful attention to details of the spring tube, the manifolding of flow, and the distribution of heat within the coil. In the case of superfluid cooling this corresponds to considerations of Kapitza conductance and balancing temperature gradient against heat flow. In the case of supercritical cooling care must be taken to balance the hydraulic flow so that the heat per mass flow is equal in all parallel channels [5]. This will likely require zoning of flow in radial regions of the coil, and balancing of the flow to control the exit temperature.

2. Q_2 , Q_3 : Block-coil Nb_3Sn quadrupoles for maximum gradient

Quadrupoles Q_2 and Q_3 are shadowed by Q_1 and thus face considerably less heat load from particles produced in collisions. We have developed designs for them that use block-coil geometry with Nb_3Sn superconductor in order to achieve maximum gradient. The aperture requirement in each quadrupole is ~ 50 mm.

The design is shown in Figure 5.

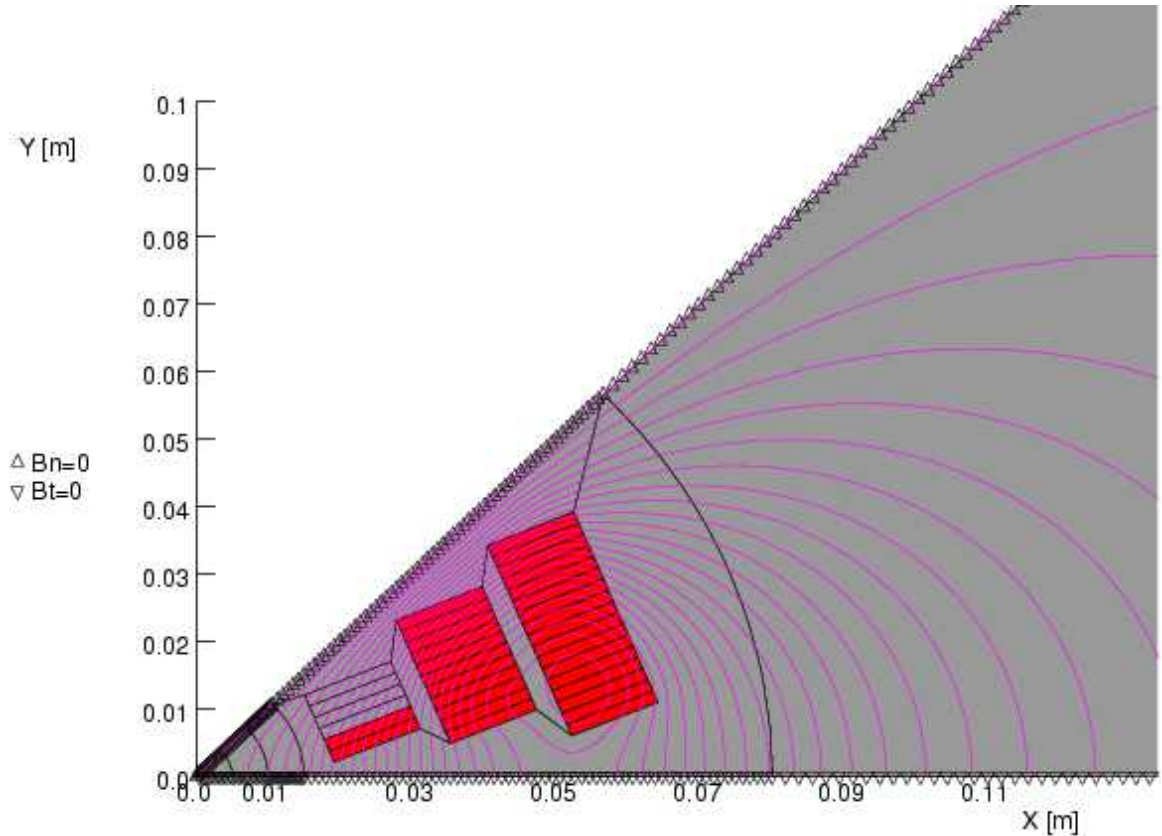


Figure 5. Block-coil Nb_3Sn Quadrupole for Q_2 , Q_3 .

3. D_1 : Levitated-pole dipole suppresses heat load from particles

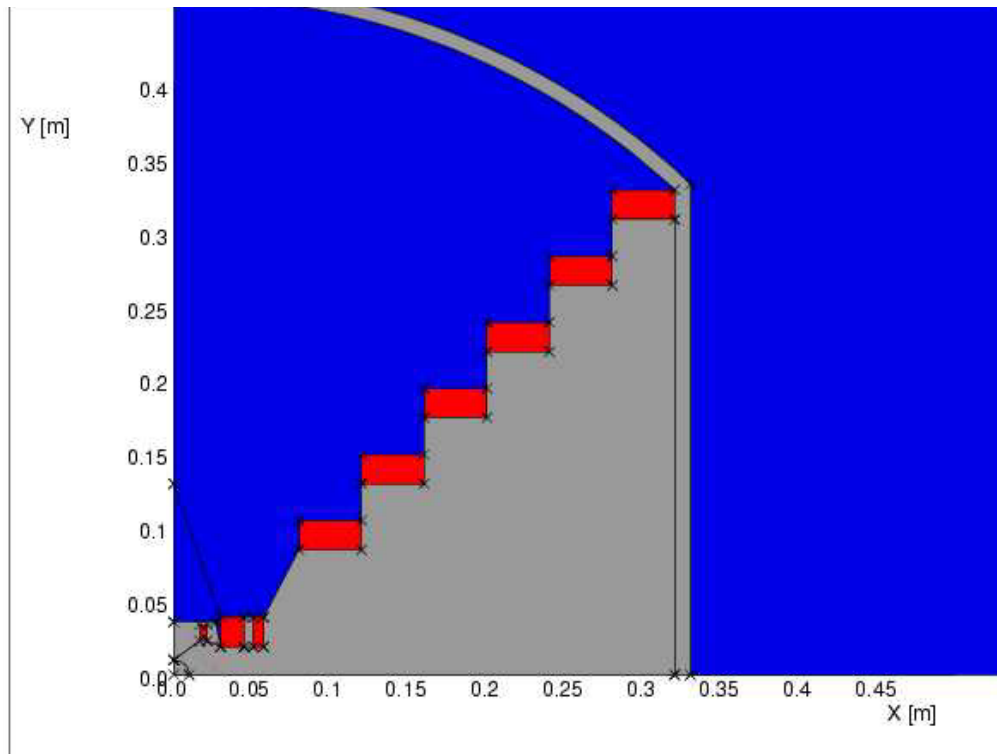


Figure 6. Levitated-pole Nb_3Sn dipole: 8.7 T central field, 56 mm bore.

4. References

¹ N.V. Mokhov, I.L. Rakhno, J.S. Kerby, J.B. Strait, "Protecting LHC IP1/IP5 components against radiation resulting from colliding beam interactions," LHC Project Report 633 (2003).

N.V. Mokhov, "The MARS Code System User's Guide," Fermilab-FN-628 (1995).

N.V. Mokhov, "Status of MARS code," Fermilab-Conf-03/053 (2003).

²

³ R. Soika *et al.*, 'Fabrication and prototype testing of a strain-tolerant Bi-2212 cable', *Physica C: Superconductivity* **341-348**, 2551-2554 (2000).

⁴ T.G. Holesinger, K.M. Marken, and J.A. Parrell, 'Microstructural development in Bi-2212 tapes by conventional and isothermal melt processing', *Proc. Appl. Superconductivity Conf.*, Virginia Beach, VA, September 17-22, 2000.

⁵ E. Hatchadourian, 'Stability and control of supercritical helium flow in the LHC circuits', *Proc. 1999 Cryogenic Engineering and International Cryogenic Materials Conference (CEC-ICMC'99)*, 12-16 July 1999, Montreal, Canada; LHC Project Report 323.